Optics Letters

Dielectric perturbations: anomalous resonance frequency shifts in optical resonators: supplement

FARHAN AZEEM,[1,2] LUKE S. TRAINOR,[1,2] PATRICK A. DEVANE,[1,2] DANIEL S. NORMAN,[1,2] ALFREDO RUEDA,[1,2] NICHOLAS J. LAMBERT,[1,2] MADHURI KUMARI,[1,2] MATTHEW R. FOREMAN,[3] AND HARALD G. L. SCHWEFEL[1,2,*]

[1] *The Dodd-Walls Centre for Photonic and Quantum Technologies, New Zealand*
[2] *Department of Physics, University of Otago, 730 Cumberland Street, Dunedin 9016, New Zealand*
[3] *Blackett Laboratory, Department of Physics, Imperial College London, Prince Consort Road, London SW7 2AZ, UK*
[*] *Corresponding author: harald.schwefel@otago.ac.nz*

Dielectric perturbations: anomalous resonance frequency shifts in optical resonators: supplemental document

Small perturbations in the dielectric environment around a high quality whispering gallery mode resonator usually lead to a frequency shift of the resonator modes directly proportional to the polarizability of the perturbation. Here, we report experimental observations of strong frequency shifts that can be opposite and even exceed the contribution of the perturbations' polarizability. The mode frequencies of a lithium niobate whispering gallery mode resonator are shifted using substrates of refractive indices ranging from 1.50 to 4.22. Both blue- and red-shifts are observed, as well as an increase in mode linewidth, when substrates are moved into the evanescent field of the whispering gallery mode. We compare the experimental results to a theoretical model by Foreman et al. [1] and provide an additional intuitive explanation based on the Goos-Hänchen shift for the optical domain.

1. REFRACTIVE INDEX OF USED SUBSTRATES

Here we provide the Table S1 of all the substrates used in the main text as well as the relevant refractive indexes.

Table S1. Substrates with varying refractive index (n_{sub}) used to observe the frequency shifts of WGM resonances.

Substrate	Symbol	n_{sub}	Reference
Germanium	Ge	4.22	[2]
Silicon	Si	3.48	[3]
Zinc Selenide	ZnSe	2.45	[2, 4]
Zinc Sulphide	ZnS	2.27	[2, 5]
Lithium Niobate (ordinary)	LN(o)	2.21	[6]
Lithium Niobate (extra-ordinary)	LN(e)	2.14	[6]
Sapphire (ordinary)	Al_2O_3(o)	1.75	[7]
Sapphire (extra-ordinary)	Al_2O_3(e)	1.74	[7]
BK7 Optical Glass	BK7	1.50	[8, 9]

2. LINEWIDTH MEASUREMENTS

Our measurements are based on measuring repeated spectra of the WGM resonator. We selected a high quality Q mode that was well coupled and isolated in the spectrum of modes. We made sure that the mode was initially critically coupled with respect to the diamond coupling prism. Then we repeatedly scanned over the mode while at the same time the substrate was moved towards the resonator. For each frequency scan a Lorentzian was fit to the mode and the linewidth and position of the mode determined. The linewidth measurement with respect
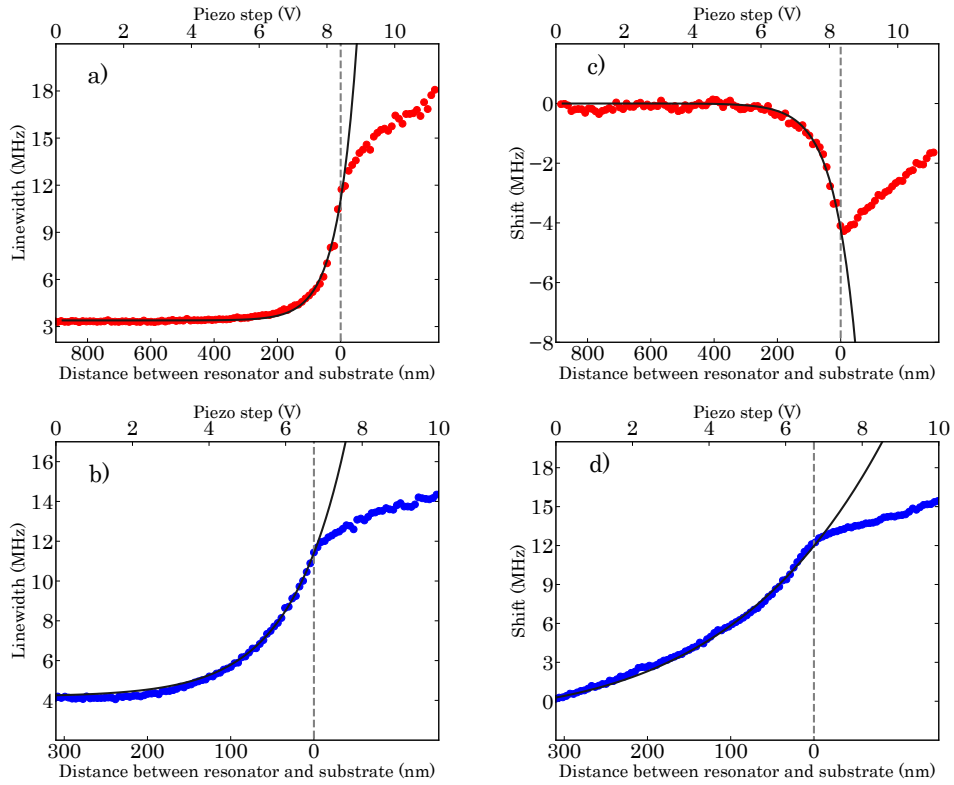
Fig. S1. Linewidth and resonant frequency shift data for the lithium niobate resonator. a,b) repeated linewidth measurements as the substrate (ZnSe, Ge) is moved towards the WGM resonator. The linewidth measurement follows a clear exponential behaviour till the WGM resonator is touched, indicated as the grey dashed line. At that point the WGM resonator is pushed by the substrate. c,d) Relative position of the resonance. This also has the expected exponential behaviour as the evanescent field is penetrated. We removed a constant linear drift in these measurements that we believe to be due to a slow external temperature drift in the setup. The measurements for ZnSe substrate a,c) are with a TM-polarized mode whereas those for Ge b,d) are with a TE-polarized mode. The distance scale is determined based on the exponential linewidth growth using a formula from Ref. [11], though its accuracy is unimportant for the measurements.

to piezo voltage/distance of the substrate is shown in Fig. S1 a,b) for the zinc selenide and the germanium substrate, respectively. We can identify the touching point by the change of the linewidth from the exponential fit [10]. The resonance position is shown in Fig. S1 c,d).

3. GOOS-HÄNCHEN SHIFT TOY MODEL

The Goos-Hänchen Shift toy model considers an that the substrate is a small (constant) effective distance d_{eff} away from the resonator, as sketched in Fig. S2. The resonance shift and mode broadening are attributed to changes in the Fresnel reflection coefficient on the resonator rim. In particular, when there is no substrate present as in Fig. S2 a), the Fresnel reflection coefficient can be written as $r_0 = -\exp(-i\Theta)$ for a real phase Θ, such that the light appears to reflect off a surface that is a distance of $\delta R = \Theta/(2k_0 n_{\text{res}} \cos\theta_i)$ away from the real surface, where k_0 is the vacuum wavevector of the light, n_{res} is the bulk refractive index of the resonator, and θ_i is the angle of incidence of the light on the boundary. The fact that the light appears to reflect off of a surface exterior to the resonator is important for eikonal approximations for whispering-gallery eigenfrequencies [12, 13]. Addition of a substrate (Fig. S2 b) changes the reflection coefficient to $r = -\exp(-i(\Theta + \delta\Theta) - \alpha)$ for real α and $\delta\Theta$, each of which depend on the effective distance between the substrate and resonator. Thus the effective boundary of the whispering-gallery resonances shifts due to the $\delta\Theta$ term and there are additional losses due to the α term. The
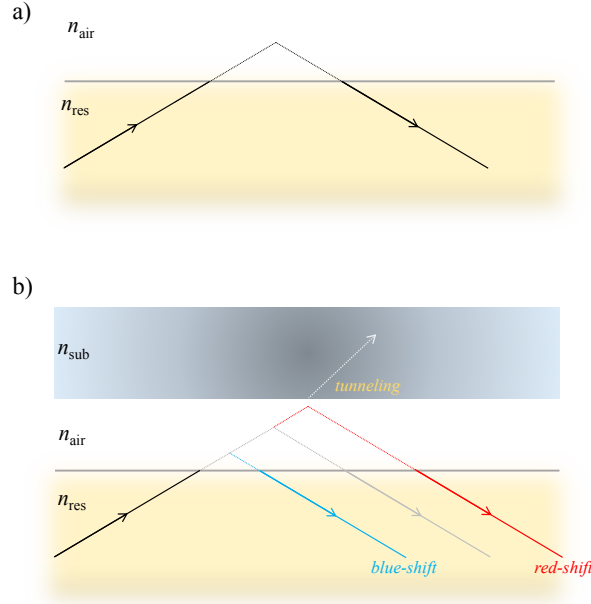
2

Fig. S2. The altered Goos-Hänchen shift at the resonator rim. a) TIR inside the resonator when a substrate is not present in its close vicinity, b) TIR inside the resonator when a substrate of refractive index n_{sub} is introduced inside its close vicinity. This results in either a blue-shift or red-shift of light, which depends on the refractive index of the substrate.

resonance shift and broadening due to the extra terms are

$$\text{resonance shift} = -\frac{c\delta\Theta}{2\cos\theta_i 2\pi n_{res}R}, \tag{S1}$$

$$\text{resonance broadening} = 2\frac{c\alpha}{2\cos\theta_i 2\pi n_{res}R}, \tag{S2}$$

where c is the speed of light in vacuum. The proportionality constant is found by considering that the resonator's effective radius increases by $\delta\Theta/(2k_0 n_{res}\cos\theta_i)$ and finding the mode frequency shift due to such a size increase. There is a factor of two in Eq. (S2) because the linewidth measures the power loss rate. The angle of incidence can be approximated by $\cos\theta_i \approx \sqrt{-\zeta_q}(m/2)^{-1/3}$, where m is the azimuthal mode number, q is the radial mode number, and $\zeta_q < 0$ is the qth root of the Airy function: $\text{Ai}(\zeta_q) = 0$. This approximation comes from analytical estimates for the mode's effective refractive index [12].

The effective distance is used as a fitting parameter to match the results of the theory by Foreman et al. [1] and it effectively absorbs the complex geometric situation of a disc-shaped resonator – whose modes have a specific spatial distribution along disc's rim – in contact with a planar substrate. The reflection coefficients were calculated using the tmm Python package [14]. As seen in Fig. 2 of the main text, the model agrees very well with the full analytical theory with the exception of TM-polarized modes when the substrate refractive index is greater than the resonator's bulk refractive index.

REFERENCES

1. M. R. Foreman, F. Sedlmeir, H. G. L. Schwefel, and G. Leuchs, "Dielectric tuning and coupling of whispering gallery modes using an anisotropic prism," J. Opt. Soc. Am. B **33**, 2177 (2016).
2. T. Amotchkina, M. Trubetskov, D. Hahner, and V. Pervak, "Characterization of e-beam evaporated Ge, YbF$_3$, ZnS, and LaF$_3$ thin films for laser-oriented coatings," Appl. Opt. **59**, A40 (2020).
3. H. H. Li, "Refractive index of silicon and germanium and its wavelength and temperature derivatives," J. Phys. Chem. Ref. Data **9**, 561–658 (1980).

4. D. T. F. Marple, "Refractive Index of ZnSe, ZnTe, and CdTe," J. Appl. Phys. **35**, 539–542 (1964).
5. M. Debenham, "Refractive indices of zinc sulfide in the 0.405–13-μm wavelength range," Appl. Opt. **23**, 2238 (1984).
6. D. E. Zelmon, D. L. Small, and D. Jundt, "Infrared corrected Sellmeier coefficients for congruently grown lithium niobate and 5 mol% magnesium oxide–doped lithium niobate," J. Opt. Soc. Am. B **14**, 3319 (1997).
7. I. H. Malitson and M. J. Dodge, "Refractive-index and birefringence of synthetic sapphire," J. Opt. Soc. Am. **62**, 1405 (1972).
8. S. H. Kim, S. H. Lee, J. I. Lim, and K. H. Kim, "Absolute refractive index measurement method over a broad wavelength region based on white-light interferometry," Appl. Opt. **49**, 910 (2010).
9. G. Ghosh, M. Endo, and T. Iwasaki, "Temperature-dependent Sellmeier coefficients and chromatic dispersions for some optical fiber glasses," J. Light. Technol. **12**, 1338–1342 (1994).
10. F. Sedlmeir, M. R. Foreman, U. Vogl, R. Zeltner, G. Schunk, D. V. Strekalov, C. Marquardt, G. Leuchs, and H. G. L. Schwefel, "Polarization-Selective Out-Coupling of Whispering-Gallery Modes," Phys. Rev. Appl. **7**, 024029 (2017).
11. M. L. Gorodetsky and V. S. Ilchenko, "Optical microsphere resonators: Optimal coupling to high-Q whispering-gallery modes," J. Opt. Soc. Am. B **16**, 147 (1999).
12. Y. A. Demchenko and M. L. Gorodetsky, "Analytical estimates of eigenfrequencies, dispersion, and field distribution in whispering gallery resonators," JOSA B **30**, 3056–3063 (2013).
13. M. Gorodetsky and A. Fomin, "Geometrical theory of whispering-gallery modes," IEEE J. Sel. Top. Quantum Electron. **12**, 33–39 (2006).
14. S. J. Byrnes, "Multilayer optical calculations," arXiv:1603.02720 [physics] (2019).